—Original—

A rat model of serous borderline ovarian tumors induced by 7,12-dimethylbenz[a]anthracene

Song-Qi CAI[1,2], Ying LI[2], Yong-Ai LI[2], Li WANG[3], Jian ZHU[4], Shu-Hui ZHAO[5], Xin LI[2] and Jin-Wei QIANG[2]

[1]*Department of Radiology, Zhongshan Hospital, Fudan University, No. 180 Fenglin Road, Xvhui District, Shanghai 200032, China*

[2]*Department of Radiology, Jinshan Hospital, Shanghai Medical College, Fudan University, No. 1508 Longhang Road, Jinshan District, Shanghai 201508, China*

[3]*Department of Pathology, Jinshan Hospital, Shanghai Medical College, Fudan University, No. 1508 Longhang Road, Jinshan District, Shanghai 201508, China*

[4]*Department of Ultrasound, The First Affiliated Hospital of Wenzhou Medical University, Nanbaixiang, Wenzhou, Zhejiang 325003, China*

[5]*Department of Radiology, Xinhua Hospital, Shanghai Jiao Tong University, No. 1665 Kongjiang Road, Yangpu District, Shanghai 200092, China*

Abstract: Serous borderline ovarian tumors (SBOTs) behave between benign cystadenomas and carcinomas, and the effective detection and clinical management of SBOTs remain clinical challenges. Because it is difficult to isolate and enrich borderline tumor cells, a borderline animal model is in need. 7,12-dimethylbenz[a]anthracene (DMBA) is capable of inducing the initiation, promotion, and progression of serous ovarian tumors. This study aims to investigate the proper dosage and induction time of DMBA for rat models of SBOTs, and explore their morphological features demonstrated by magnetic resonance (MR) imaging and molecular genetic characteristics. Rats were randomly divided into six groups (1 mg/70 D, 2 mg/70 D, 3 mg/70 D, 2 mg/50 D, 2 mg/90 D, and 2 mg/110 D). The 3 mg/70 D group induced the most SBOTs (50.0%, 12/24). The micropapillary projections were shown on MR imaging, which was the characteristic of SBOTs. The Cyclin D1 characterizing an early pathogenetic event strongly expressed in induced serous benign tumors (SBTs). The immunoreactivity staining scores of P53 expression significantly increased from SBTs, SBOTs to serous ovarian carcinomas (SCAs), which elucidate that P53 might be a promising biomarker to grade serous ovarian tumors. Based on morphological and molecular genetic similarities, this rodent SBOT model was suitable for investigating the pathogenesis of serous ovarian tumors and developing an early detection strategy.

Key words: animal model, dimethylbenz[a]anthracene, ovarian tumor, serous borderline tumor, Sprague-Dawley rat

Introduction

Ovarian borderline tumors are a puzzling group of neoplasms, which behave between benign cystadenomas and carcinomas. They are characterized pathologically by irregular papillae, cellular proliferation and nuclear atypia, but without obviously destructive stromal invasion [6]. Serous tumors take up about 60% of all ovar-

ian epithelial tumors; therefore, serous borderline ovarian tumors (SBOTs) are the major focus [6]. They have significantly better prognosis even when they present as advanced stage tumors and are inadequately treated [14]. They are supposed to be the precursors of type I serous ovarian carcinomas (SCAs) [9]. However, their pathogenesis is unclear, and clinical management is controversial, and effective detection and clinical management of SBOTs remains a clinical challenge [3]. Studies on SBOTs can benefit early detection of SBOTs and develop proper prevention strategies of ovarian cancers.

However, it is difficult to isolate and enrich borderline tumor cells, because unlike most solid tumors, SBOT cells are arranged as a single layer and overlie abundant stroma [18]. Animal models are in need to extrapolate to SBOTs occurring in women. 7,12-dimethylbenz[a] anthracene (DMBA) is a well-known polycyclic aromatic carcinogen that is capable of inducing the initiation, promotion and progression of tumors [12]. During the development from neoplasms to massive tumors, Stewart *et al.* observed a rat ovarian borderline tumor [22]. Moreover, the mean maximum diameter (MMD) of the induced tumors by embedding high purity DMBA cloth strip on rats ovaries was approximately 1.5 cm, the size of which was feasible for *in vivo* image monitoring [4]. While most previous studies of these models focused on ovarian cancers, SBOTs had rarely been investigated. In the present study, different dosages of DMBA and induction times were investigated to identify the most effective combination to induce SBOTs in rats. The morphological and genetic molecular characteristics of induced SBOTs were explored, and compared to those of human beings.

Materials and Methods

This study was approved by the Institutional Review Board of local hospital, and performed in strict accordance with the Guide for the Care and Use of Laboratory Animals of the National Science and Technology Committee of China. Every effort was made to minimize animal suffering.

Animals and in vivo treatments

One hundred and eighty female Sprague-Dawley rats weighing 150–200 g, with ages ranging from 5 to 7 weeks (Shanghai Experimental Animal Co., Ltd., SCXK[SH] 2012-0006), were acclimated to the animal room for one week before surgery. According to the results of preliminary experiment, rats were divided into six groups with 30 rats in each group, and the DMBA dosages (mg) and induction times (D, days) in the six groups were 1 mg/70 D, 2 mg/70 D, 3 mg/70 D, 2 mg/50 D, 2 mg/90 D, and 2 mg/110 D.

DMBA cloth strip preparation

DMBA (Sigma Chemical Co., St. Louis, MO, USA) with 99% purity was heated to the fusion point of 124°C. Cloth strips (0.25 cm × 0.5 cm, 0.5 cm × 0.5 cm, 0.75 cm × 0.5 cm) were immersed in the melted DMBA and contained 1 mg, 2 mg, and 3 mg of carcinogen on average, as calibrated by a micro-chemical balance.

DMBA application to the ovary

The surgical procedures were referred to previous study [4]. Rats were anesthetized by intraperitoneal injection of 10% chloral hydrate at 3 ml/kg. Then, both ovaries were surgically exposed and packed with a DMBA-coated cloth strip or a saline-coated cloth strip (serving as the control). The surgical area was closed with the surrounding fatty substance. An antibiotic (10^5 units of benzylpenicillin potassium) was administered intraperitoneally for prophylaxis against infection before the abdominal wall was closed.

Magnetic resonance (MR) imaging scanning and immunohistochemistry

All rats underwent MR imaging scanning to detect lesions every two weeks under anesthesia. Images were acquired with 3.0 T MR scanner (Verio, Siemens, Erlangen, Germany), with an animal coil. The following sequences were obtained: axial spin-echo (SE) T1-weighted imaging (T1WI) (repetition time [TR]/echo time [TE] = 7.29 / 2.28 ms); turbo SE axial, sagittal and coronal T2-weighted imaging [T2WI] with fat saturation [TR/TE = 2,500 / 93 ms], and turbo SE T2WI (TR/TE = 8,000 / 98 ms). The scanning parameters were as follows: slice thickness 1–2 mm; gap 1.5 mm; matrix 224 × 370; field of view 80 mm × 80 mm; and excitations 4.

On MR images, the tumors size, configuration (cystic, solid, or cystic-solid), wall and septum thickness, size of solid components, nodules or papillary projections were analyzed.

The rats were euthanized by i.v. administration 1 ml 10% chloral hydrate, then dissected and examined for gross abnormalities. Macroscopic specimens of altered

Table 1. The histologic features of different subtypes and grades in 7,12-dimethylbenz[a]anthracene (DMBA) induced ovarian tumors

	Histologic features
Tumor subtype	
Serous	Cuboidal to columnar cells resembleing fallopian tube epithelium
Mucinous	Resembling gastric foveolar-type or intestinal epithelium containing goblet cells
Endometrioid	Simple or pseudostratified epithelium overlying endometrial stroma and is associated with haemorrhage
Clear cell	Composed of clear, eosinophilic, hobnail cells
Histologic grade	
Cyst or cystadenoma	Simple epithelial composed of flat or columnar cells
Borderline tumor	Pseudostratified epithelium (<3 lines), cells containing moderately enlarged and atypical nuclei, and without destructive stromal invasion
Carcinoma	Significant nuclear atypia, different patterns of invasion often coexist

organs, tissues and entire reproductive tracts were removed and fixed in 10% (v/v) neutral buffered formalin overnight. The specimens were dissected into sections at 1–3 mm interval by L.W., who has 15 years of experience in human and murine gynecological pathology.

For histological analysis, 3-μm sections were cut for hematoxylin and eosin (H&E) and immunohistochemical staining. The epithelial tumors were subtyped, and further subdivided into benign lesions (cyst and cystadenoma), borderline ovarian tumors and carcinomas according to the histopathological characteristics of the neoplastic cells (Table 1).

Cyclin D1 and P53 was stained using the corresponding monoclonal antibody (clone-EPR2241 and clone-EPR17974, Abcam, Cambridge, UK) according to established methods [16]. Immunohistochemical analyses of Cyclin D1 and P53 expression were performed by Allred method. The proportion of positive cells was scored as the following: 0, 0% no positive cells; 1, ≤1% positive cells; 2, 1–10% positive cells; 3, 11–33% positive cells; 4, 34–66% positive cells; and 5, ≥67%. The intensity of positive cells was assigned as follows: 0, no staining; 1, weak staining; 2, moderate staining; and 3, strong staining. Finally, we defined the cases with the summed score.

Statistical analysis

Statistical analysis was performed with SPSS 22.0 for Mac (SPSS Inc., Chicago, IL, USA). All variables were expressed as the mean value±standard deviation or median (interquartile range, 25th percentile and 75th percentile). Fisher's exact test was performed to compare the difference in configuration. The differences in tumor and solid component size and wall, septum thickness, and Cyclin D1 and P53 expression among the three

groups were compared using one-way ANOVA or Kruskal-Wallis. $P<0.05$ was considered statistically significant.

Results

Incidence of ovarian neoplasia and histology

Overall, 162 DMBA-treated ovaries developed tumors (18 rats died before the experiment was completed), and no tumors developed in the control group. Serous tumors accounted for 87.7% (142/162) of all the tumors. The other tumors included two sarcomas, and other epithelial subtypes (mucinous, endometrioid and clear cell tumors). The distribution of serous lesions among the three differentiation groups is shown in Table 2. Serous benign tumors (SBTs), SBOTs and SCAs counted for 54.2% (77/142), 33.1% (47/142) and 12.7% (18/142) of tumors, respectively (Fig. 1). The 3 mg/70 D group developed the most SBOTs (50.0%, 12/24). Seventy-nine of 142 serous tumors were cystic, 12 were cystic-solid, and 51 were solid (Table 3). The configuration of the three groups was significantly different. Most cystic lesions were SBTs (62.0%, 49/79), and most cystic-solid tumors were SBOTs (58.3%, 7/12). No peritoneal implants were found in any of the rats.

The histologic grades of induced tumors at different termination time and dosage is shown in Table 2. The dosage and induction time were positively correlated with ovarian tumor differentiation (r=0.422, P=0.000; r=0.307, P=0.000, respectively)

MR findings

SBOTs had four MR imaging morphological patterns which were histopathologically confirmed as follows
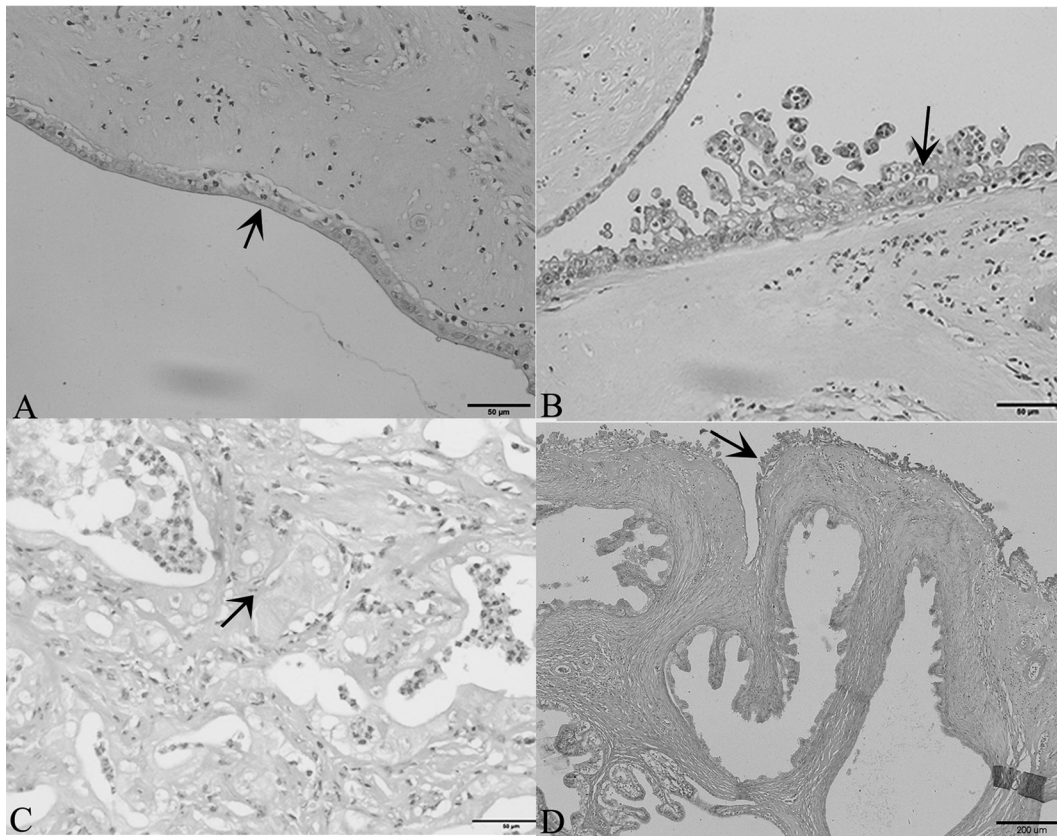
Fig. 1. Histopathology of serous tumors with different grades. A. Serous adenoma lined by non-stratified columnar cells (arrow); B. Serous borderline tumor lined by stratified columnar cells with papillae (arrow), containing a moderate nuclear pleomorphism; C and D. Serous carcinoma with slit-like spaces (C, arrow), high-grade nuclear atypia, and involvement of the fallopian tube surface (D, arrow) (H&E, A, B, C×400; D×100).

Table 2. 7,12-dimethylbenz[a]anthracene (DMBA) induced ovarian tumors in the different time and dosage groups

Time & dosage	Others (n, %)	SBT (n, %)	SBOT (n, %)	SCA (n, %)
DMBA 2 mg				
50 d	7/28 (25.0)	16/28 (57.1)	5/28 (17.9)	0/28 (0.0)
70 d	4/27 (14.8)	13/27 (48.1)	9/27 (33.3)	1/27 (3.7)
90 d	0/29 (0.0)	12/29 (41.4)	9 /29(31.0)	8/29 (27.6)
110 d	2/27 (7.4)	9/27 (33.3)	8/27 (29.6)	8/27 (29.6)
DMBA 70 d				
1 mg	5/27 (18.5)	18/27 (66.7)	4/27 (14.8)	0/27 (0.0)
2 mg	4/27(14.8)	13/27 (48.1)	9/27 (33.3)	1/27 (3.7)
3 mg	2/24 (8.3)	9/24 (37.5)	12/24 (50.0)	1/24 (4.2)

Others including mucinous, endometrioid, clear cell tumors and sarcoma; SBT: serous benign tumor; SBOT: serous borderline ovarian tumor; SCA: serous carcinoma.

Table 3. The configurations of different grading tumors

	SBT	SBOT	SCA	P	P_1	P_2	P_3
Cystic (n=79)	49	22	8	0.000	0.000	0.000	0.008
Cystic-solid (n=12)	4	7	1	0.034	0.414	0.317	0.027
Solid (n=51)	22	21	8	0.005	1.000	0.004	0.008

P_1: SBT vs SBOT; P_2: SBT vs SCA; P_3: SBOT vs SCA.
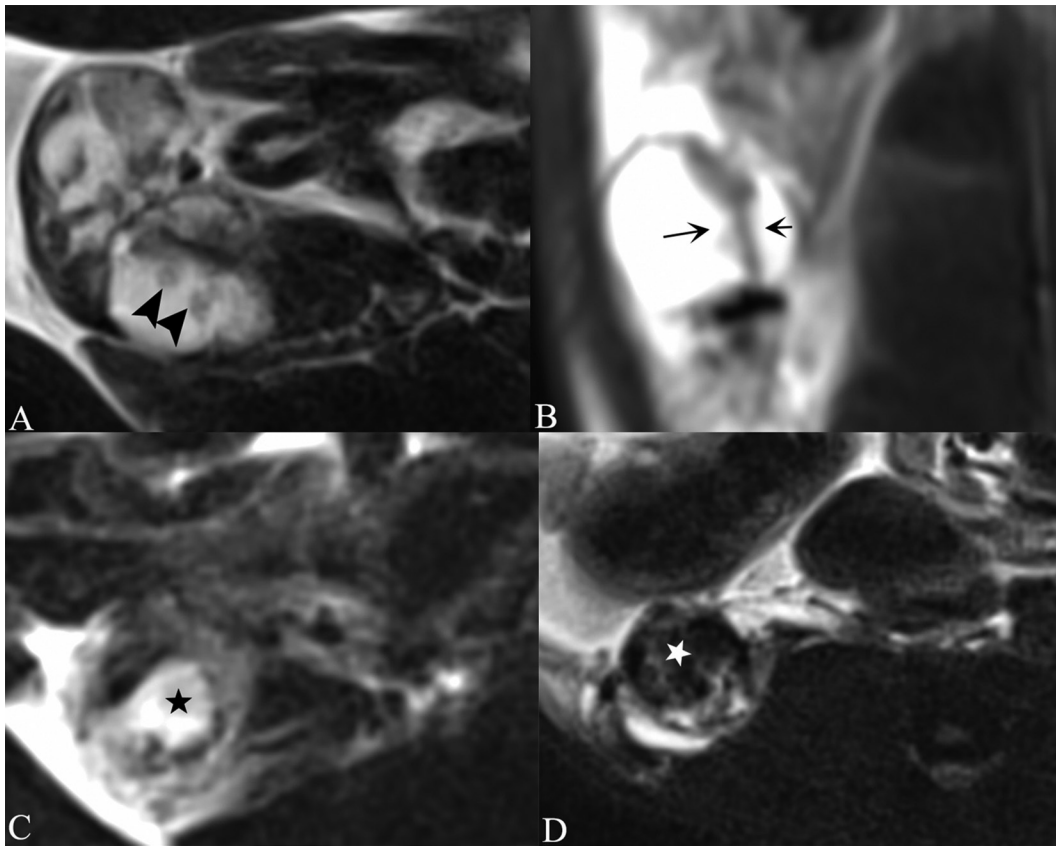
Fig. 2. Four magnetic resonance (MR) imaging morphological patterns of rodent serous borderline ovarian tumors (SBOTs) confirmed by gross pathological specimen. A. A cystic SBOT with papillary: the intracystic papillary projections were low signal intensity on axial T2WI (black arrowheads); B. A multilocular SBOT with thickened septa: the coronal T2WI showed a bilocular cystic tumor with a thickened septum (black arrows); C. A cystic-solid SBOT: the axial T2WI showed a cystic-solid tumor with thickened cystic wall and a cyst in the center (black star); D. A solid SBOT: the solid mass was isointense on axial T2WI (white star) without a cystic component.

(Figs. 2 and 3): (i) mainly cystic with or without papillary; (ii) multilocular with or without thickened wall or septa; (iii) cystic-solid; and (iv) solid. The MMDs of tumor size of SBTs, SBOTs and SCAs were 11.65 ± 2.69 mm (7.0–19.1 mm), 13.20 ± 2.65 mm (8.4–20.1 mm) and 13.48 ± 2.51 mm (10.6–20.1 mm), respectively (SBTs vs SBOTs, $P=0.009$; SBOTs vs SCAs, $P=0.716$; SCAs vs SBTs, $P=0.015$) (Fig. 4A). The MMDs of the solid components were 2.40 ± 0.96 mm (1.5–4 mm), 2.86 ± 1.55 mm (1.5–5 mm) and 10.17 ± 14.88 mm (2–40 mm) in SBTs, SBOTs and SCAs, respectively (SBTs vs SBOTs vs SCAs, $P=0.249$). The MMDs of the cystic wall or septum were 0.85 ± 0.49 mm (0.5–2.0 mm), 1.96 ± 0.72 mm (1.0–3.0 mm) and 2.50 ± 1.35 mm (1.0–4.0 mm), respectively (SBTs vs SBOTs, $P=0.000$; SBOTs vs SCAs, $P=0.140$; SBTs vs SCAs, $P=0.000$) (Fig. 4B).

Immunohistochemistry

To investigate the pathogenesis of SBOTs, expression of Cyclin D1 and P53 were analyzed. Fifteen SBTs, 17 SBOTs and 17 SCAs were included. The immunoreactivity staining scores of Cyclin D1 was 7 (6, 7) for SBTs, 2 (0, 7) for SBOTs, and 2 (0, 5) for SCAs. There was a significant difference in Cyclin D1 expression between SBOTs and SBTs ($P=0.014$), while no difference was found between SBOTs and SCAs ($P=0.715$). The immunoreactivity staining scores of P53 was 0.93 ± 0.33 for SBTs, 2.89 ± 0.49 for SBOTs, and 4.71 ± 0.54 for SCAs. Significant differences were found among the three groups (SBTs vs SBOTs, $P=0.006$; SBTs vs SCAs, $P=0.000$; SBOTs vs SCAs, $P=0.008$) (Table 4 and Fig. 5).
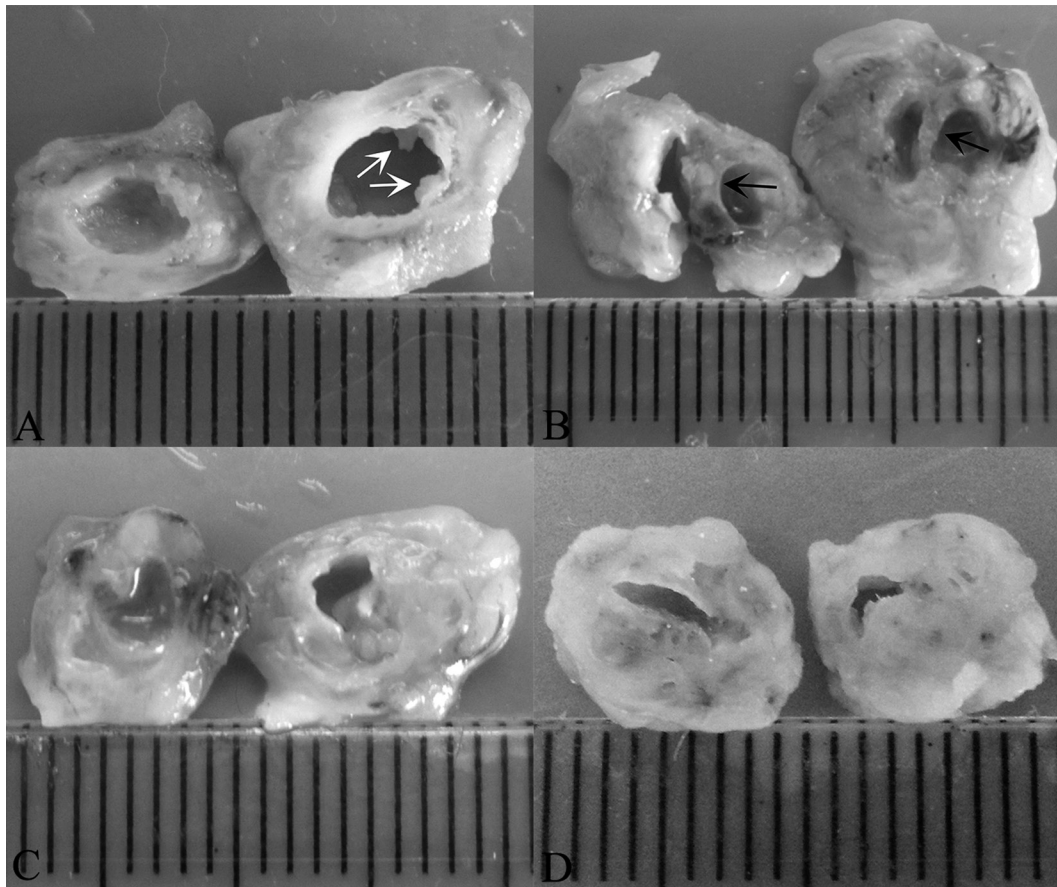
Fig. 3. Gross pathological specimen of rodent serous borderline ovarian tumors (SBOTs). A. The cystic SBOT with intracystic papillary projections (white arrows); B. The SBOT including two loculi with a thickened septum (black arrows); C. The cystic-solid SBOT with the solid component accounting for more than 1/3 of the tumor; D. The solid SBOT without a cystic component (1 mm for scale interval).
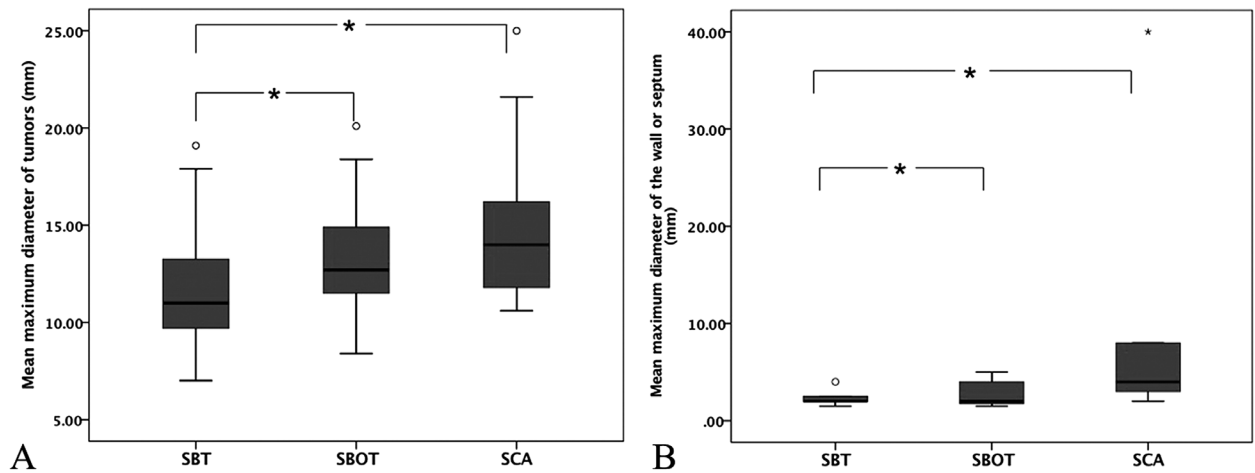

Fig. 4. Boxplots showing the mean maximum diameter (MMD) of the tumors and cystic wall or septum in three tumor grades. The tumor size (A) and cystic wall or septum thickness (B) increased progressively with increasing tumor grade; there is no difference between SBOT and SCA (*$P<0.05$).

Table 4. The immunoreactivity staining scores of Cyclin D1 and P53 of different grading tumors

	SBT	SBOT	SCA	P	P_1	P_2	P_3
Cyclin D1	7(6, 7)	2(0, 7)	2(0, 5)	0.003	0.014	0.001	0.715
P53	0.93 ± 0.33	2.89 ± 0.49	4.71 ± 0.54	0.000	0.006	0.000	0.008

P_1: SBT vs SBOT; P_2: SBT vs SCA; P_3: SBOT vs SCA.
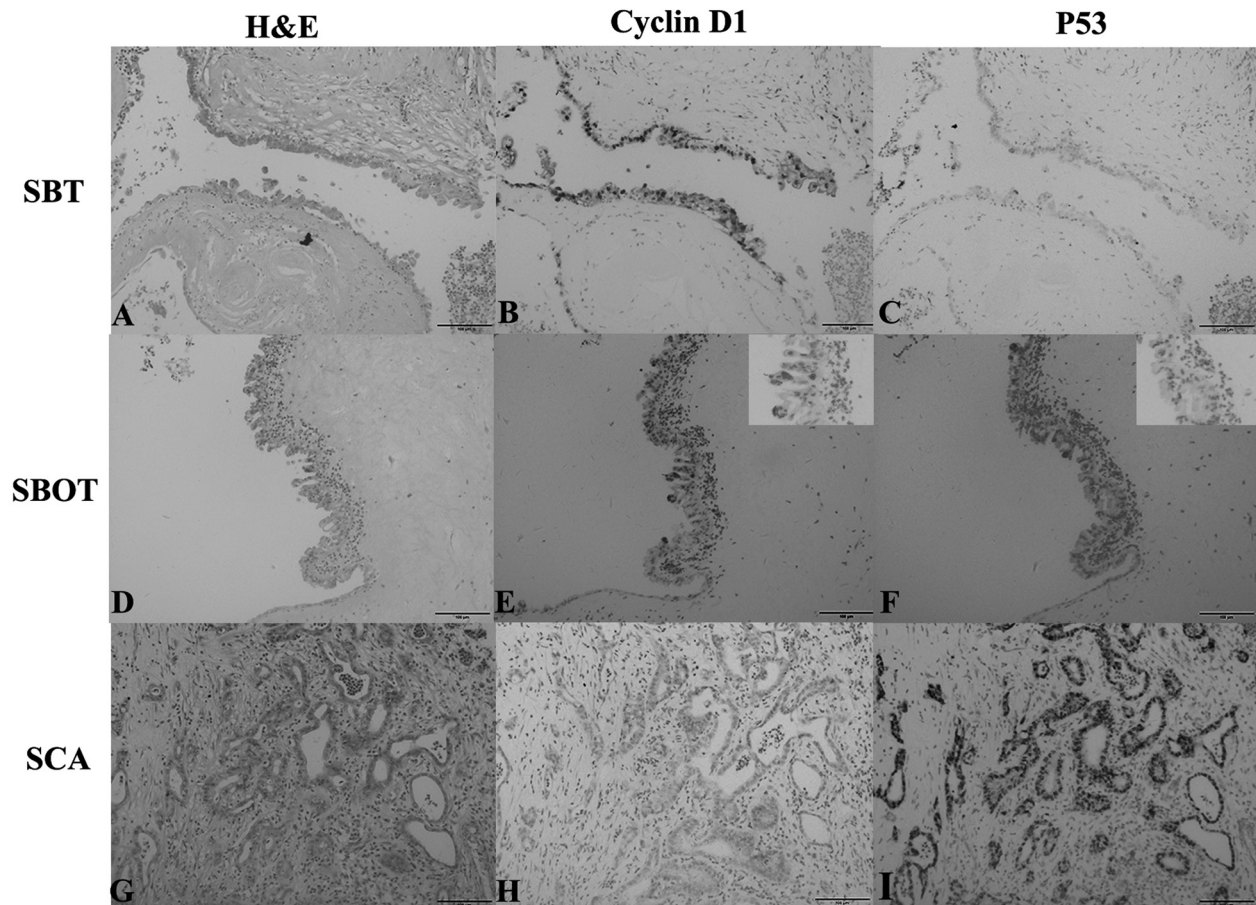
Fig. 5. The immunoreactivity staining scores of Cyclin D1 and P53 in different serous tumor grades. Cyclin D1 is strongly expressed in serous benign tumor (B), weakly in borderline tumor (E), and not in carcinoma (H) (200×). P53 is strongly expressed in the carcinoma (I), moderately in borderline tumor (F), but not in benign tumor (C) (200×).

Discussion

Ovarian cancer is composed of a heterogeneous group of tumors. They are classified into serous, mucinous, endometrioid, clear cell, and Brenner types. Serous ovarian tumor is the most common pathological subtype, accounting up to 60% in human [1]. In present study, serous tumors accounted up to 87.7% of all tumors by embedding a DMBA-coated cloth strip on the ovary. In the similar experiment conducted by Huang *et al.*, epithelial tumors accounted for 93.75% [4]. But they did not investigate the subtypes of the induced epithelial tumors.

In this study, we successfully established the rodent SBOT model and found that combining 3 mg of DMBA and a 70-day induction time was the most effective in the induction of SBOTs (50%). In theory, DMBA is capable of inducing the initiation, promotion and progression of tumors by an optimal period of ovarian instillation and proper dosage [10, 11]. Consistently, we found that the dosages and induction times were correlated with the histologic grades of the ovarian tumors. To the best

of our knowledge, this is the first study with respect to establishing the SBOT model.

As expected, SBTs counted for the most of cystic lesions, and SBOTs for the most of cystic-solid tumors in this study. As known to all, most human epithelial tumors are primarily cystic, and a varying proportion of solid components strongly indicates potential malignancy (i.e. SBOTs and SCAs) [5]. Generally, histologically identified rats' SBOTs have similar MRI morphological subtypes to those of humans, which is also divided into four subtypes: unilocular cysts with papillary projections, minimally septate cysts with papillary projections, markedly septate cysts (over five septa) with plaque-like excrescences and predominantly solid lesions with exophytic papillary projections [1, 7, 25]. As we know, micropapillary projection was a characteristic of SBOTs, which had been reported in previous researches [5, 8, 15, 23]. This architecture was also found in the rat SBOT model. The tumor size, septum thickness and the size of solid components of induced SBOTs and early SCAs (without metastases) were no difference. It is also a clinical challenge to differentiate borderline tumors from stage I cancers: deSouza *et al.* found neither the septum thickness and size of solid components allowed confident differentiation between borderline tumors and stage I cancers [2]. Our animal model may be helpful in the further investigation of this issue.

Cyclin D1 is a cell cycle phase marker involved in the G1/S transition, which is associated with the mutations of KRAS and BRAF [18]. Recent studies have verified the original finding and further showed that mutations in KRAS and BRAF characterize SBOTs and low-grade serous carcinomas [19–21]. In the present study, we found that Cyclin D1 was expressed in SBOTs and the early stage of SCAs. This elucidated that the induced SBOTs may yield similar molecular genes with those of humans. The result showed that Cyclin D1 also expressed in SBTs, and higher level expression was observed in SBTs than those in SBOTs and SCAs. The reason might be that Cyclin D1 is an early pathogenetic event with epithelial ovarian cancer [19, 21, 24].

P53 tumor suppressor gene plays a central role in the maintenance of normal cell growth and differentiation, which is considered to be the most common genetic alteration in ovarian cancer [17]. In the present study, P53 demonstrated significantly different expression in SBTs, SBOTs and SCAs, with SCAs showing the highest level of P53 expression. Furthermore, P53 showed sig-

nificant difference between SBOTs and SCAs. Similar results in humans were observed in the study conducted by Ozer H *et al.* [13]. In that study, they found that the level of P53 expression was correlated with the invasiveness of ovarian tumors, and acted as a potential predictor for malignant tumors (i.e. SBOTs and SCAs). The results of this study indicated that P53 might be a promising biomarker not only in the differentiation between benign and malignant tumors, but also in the differentiation between SBOTs and SCAs. However, the specific threshold values and how it is related to patient's clinical staging need further investigation.

Conclusion

In summary, SBOTs were most effectively induced at 70 days by embedding 3 mg of high purity DMBA cloth strips on the rodent ovarian surface. Based on morphological and molecular genetic similarities, this rodent SBOT model is adequate for pathogenesis and early detection studies.

References

1. Bent, C.L., Sahdev, A., Rockall, A.G., Singh, N., Sohaib, S.A. and Reznek, R.H. 2009. MRI appearances of borderline ovarian tumours. *Clin. Radiol.* 64: 430–438. [Medline] [CrossRef]
2. deSouza, N.M., O'Neill, R., McIndoe, G.A., Dina, R. and Soutter, W.P. 2005. Borderline tumors of the ovary: CT and MRI features and tumor markers in differentiation from stage I disease. *AJR Am. J. Roentgenol.* 184: 999–1003. [Medline] [CrossRef]
3. du Bois, A., Trillsch, F., Mahner, S., Heitz, F. and Harter, P. 2016. Management of borderline ovarian tumors. *Ann. Oncol.* 27:(Suppl 1): i20–i22. [Medline] [CrossRef]
4. Huang, Y., Jiang, W., Wang, Y., Zheng, Y., Cong, Q. and Xu, C. 2012. Enhanced efficacy and specificity of epithelial ovarian carcinogenesis by embedding a DMBA-coated cloth strip in the ovary of rat. *J. Ovarian Res.* 5: 21. [Medline] [CrossRef]
5. Khashper, A., Addley, H.C., Abourokbah, N., Nougaret, S., Sala, E. and Reinhold, C. 2012. T2-hypointense adnexal le-

sions: an imaging algorithm. *Radiographics* 32: 1047–1064. [Medline] [CrossRef]

6. Longacre, T.A. and Wells, M. 2014. Serous tumors. pp. 15–24. In: WHO classification of tumours of female reproductive organs (4rd) (Kurman, R.J., Carcangiu, M.L., Herrington, C.S., and Young, R.H.), Kodansha, Lyon.

7. Morotti, M., Menada, M.V., Gillott, D.J., Venturini, P.L. and Ferrero, S. 2012. The preoperative diagnosis of borderline ovarian tumors: a review of current literature. *Arch. Gynecol. Obstet.* 285: 1103–1112. [Medline] [CrossRef]

8. Naqvi, J., Nagaraju, E. and Ahmad, S. 2015. MRI appearances of pure epithelial papillary serous borderline ovarian tumours. *Clin. Radiol.* 70: 424–432. [Medline] [CrossRef]

9. Nik, N.N., Vang, R., Shih, IM. and Kurman, R.J. 2014. Origin and pathogenesis of pelvic (ovarian, tubal, and primary peritoneal) serous carcinoma. *Annu. Rev. Pathol.* 9: 27–45. [Medline] [CrossRef]

10. Nishida, T., Oda, T., Sugiyama, T., Nishida, T., Nishimura, H., Tsunawaki, A. and Yakushiji, M. 1982. Squamous cell carcinoma arising from an epidermoid cyst in the ovary of a rat treated with 7,12-dimethylbenz[a]anthracene. *Gan* 73: 153–157. [Medline]

11. Nishida, T., Sugiyama, T., Katabuchi, H., Yakushiji, M. and Kato, T. 1986. Histologic origin of rat ovarian cancer induced by direct application of 7,12-dimethylbenz(a)anthracene. *Nippon Sanka Fujinka Gakkai Zasshi* 38: 570–574. [Medline]

12. Nishida, T., Sugiyama, T., Kataoka, A., Ushijima, K. and Yakushiji, M. 1998. Histologic characterization of rat ovarian carcinoma induced by intraovarian insertion of a 7,12-dimethylbenz[a]anthracene-coated suture: common epithelial tumors of the ovary in rats? *Cancer* 83: 965–970. [Medline] [CrossRef]

13. Ozer, H., Yenicesu, G., Arici, S., Cetin, M., Tuncer, E. and Cetin, A. 2012. Immunohistochemistry with apoptotic-anti-apoptotic proteins (p53, p21, bax, bcl-2), c-kit, telomerase, and metallothionein as a diagnostic aid in benign, borderline, and malignant serous and mucinous ovarian tumors. *Diagn. Pathol.* 7: 124. [Medline] [CrossRef]

14. Park, J.Y., Kim, D.Y., Kim, J.H., Kim, Y.M., Kim, Y.T. and Nam, J.H. 2009. Surgical management of borderline ovarian tumors: The role of fertility-sparing surgery. *Gynecol. Oncol.* 113: 75–82. [Medline] [CrossRef]

15. Park, S.B., Kim, M.J., Lee, K.H. and Ko, Y. 2018. Ovarian serous surface papillary borderline tumor: characteristic imaging features with clinicopathological correlation. *Br.*

J. Radiol. 91: 20170689 [Epud ahead of print]. [Medline] [CrossRef]

16. Penuel, E., Li, C., Parab, V., Burton, L., Cowan, K.J., Merchant, M., Yauch, R.L., Patel, P., Peterson, A., Hampton, G.M., Lackner, M.R. and Hegde, P.S. 2013. HGF as a circulating biomarker of onartuzumab treatment in patients with advanced solid tumors. *Mol. Cancer Ther.* 12: 1122–1130. [Medline] [CrossRef]

17. Schuijer, M. and Berns, E.M. 2003. TP53 and ovarian cancer. *Hum. Mutat.* 21: 285–291. [Medline] [CrossRef]

18. Shih, IM. and Kurman, R.J. 2005. Molecular pathogenesis of ovarian borderline tumors: new insights and old challenges. *Clin. Cancer Res.* 11: 7273–7279. [Medline] [CrossRef]

19. Sieben, N.L., Macropoulos, P., Roemen, G.M., Kolkman-Uljee, S.M., Jan Fleuren, G., Houmadi, R., Diss, T., Warren, B., Al Adnani, M., De Goeij, A.P., Krausz, T. and Flanagan, A.M. 2004. In ovarian neoplasms, BRAF, but not KRAS, mutations are restricted to low-grade serous tumours. *J. Pathol.* 202: 336–340. [Medline] [CrossRef]

20. Singer, G., Oldt, R. 3rd., Cohen, Y., Wang, B.G., Sidransky, D., Kurman, R.J. and Shih, IM. 2003. Mutations in BRAF and KRAS characterize the development of low-grade ovarian serous carcinoma. *J. Natl. Cancer Inst.* 95: 484–486. [Medline] [CrossRef]

21. Singer, G., Kurman, R.J., Chang, H.W., Cho, S.K. and Shih, IM. 2002. Diverse tumorigenic pathways in ovarian serous carcinoma. *Am. J. Pathol.* 160: 1223–1228. [Medline] [CrossRef]

22. Stewart, S.L., Querec, T.D., Ochman, A.R., Gruver, B.N., Bao, R., Babb, J.S., Wong, T.S., Koutroukides, T., Pinnola, A.D., Klein-Szanto, A., Hamilton, T.C. and Patriotis, C. 2004. Characterization of a carcinogenesis rat model of ovarian preneoplasia and neoplasia. *Cancer Res.* 64: 8177–8183. [Medline] [CrossRef]

23. Tanaka, Y.O., Okada, S., Satoh, T., Matsumoto, K., Oki, A., Nishida, M., Yoshikawa, H., Saida, T. and Minami, M. 2011. Ovarian serous surface papillary borderline tumors form sea anemone-like masses. *J. Magn. Reson. Imaging* 33: 633–640. [Medline] [CrossRef]

24. Worsley, S.D., Ponder, B.A. and Davies, B.R. 1997. Overexpression of cyclin D1 in epithelial ovarian cancers. *Gynecol. Oncol.* 64: 189–195. [Medline] [CrossRef]

25. Ma, F.H., Zhao, S.H., Qiang, J.W., Zhang, G.F., Wang, X.Z. and Wang, L. 2014. MRI appearances of mucinous borderline ovarian tumors: pathological correlation. *J. Magn. Reson. Imaging* 40: 745–751. [Medline] [CrossRef]